Journal of Opto-Electro-Medic Science

Vol. 1, No. 1, February 2025, pp. 15-20, DOI: 10.59190/joems.v1i1.299

JOEMS

PUBLISHED BY

LSPRAR

Application of stereoelectroencephalography utilising single pulse electrical stimulation method for brain connectivity: A review

Raudatul Jannah
Department of Physics, Universitas Riau, Pekanbaru 28293, Indonesia

ABSTRACT

Stereoelectroencephalography (SEEG) is a technique that allows direct observation of brain activity through electrodes implanted into the brain. This study utilized the single pulse electrical stimulation (SPES) method to explore brain connectivity structurally, functionally, and effectively. Results showed that SEEG with SPES was able to record pulse evoked potentials (PEP) indicating connections between neurons with high accuracy. Connectivity analysis identified PEP features, such as C1 peak amplitude, that significantly correlated with structural connection strength. However, connectivity models show limitations in areas with low connectivity or complex anatomy, such as brain sulci. In addition, the three-dimensional network topology showed improved conductivity resolution around the electrodes. This study underscores the need to improve methodologies to improve precision and resolution in brain connectivity assessment, as well as stimulation procedures.

ARTICLE INFO

Article history:

Received Dec 8, 2024
Revised Jan 11, 2025
Accepted Feb 14, 2025

Keywords:

Brain Connectivity
Pulse Evoked Potentials
SEEG
SPES
Structural Connections

* **Corresponding Author**
E-mail address: raudatul.jannah0178@student.unri.ac.id

1. INTRODUCTION

The brain functions to oversee, regulate, and sustain the entire body to ensure survival. The brain produces connectomes at multiple spatial scales that form a comprehensive map of neuronal connections (circuits) throughout the brain. It is susceptible to imbalance, resulting in the disruption of electrical impulses in the brain. The analysis of brain networks and information processing include anatomical, functional, and effective connection. Recruiting the appropriate networks in an ideal manner continues to be a primary objective of stimulation-based therapies. Brain networks likely consist of spatially distributed, yet functionally and physically coupled nodes that enable cellular communication [1].

A contributing element to the dispersion of errors among brain regions is the significant disparity in potentials between nearby electrodes, which undermines the efficacy of numerical models. Significant potential differences in small isolated spatial regions indicate steep gradients with low localised conductivity values. Electrodes situated in the grey matter proximal to the sulcus exhibited more model inaccuracies. The results indicate that anatomical characteristics may account for some variability in model error, including intricate cortical folding patterns surrounding electrodes that enhance PEP features, such as alterations in component amplitude resulting from traversing distinct yet spatially adjacent regions due to variations in dipole geometry [2].

2. THEORITICAL REVIEW

2.1. Stereoelectroencephalography (SEEG)

SEEG is utilised in the pre-surgical assessment of epileptic patients and is becoming adopted in medical institutions globally. The SEEG electrodes have dual purposes: they facilitate recording and function as single pulse electrical stimulation (SPES) for neural networks, enabling functional brain mapping and seizure induction. The SEEG measurements are affected by the stimulation and recording contact points either on the same electrode shaft or on two distinct shafts [3].

2.2. Magnetic Resonance Imaging (MRI)

MRI is a widely utilised imaging technique for examining structural alterations. MRI is regarded as a significant diagnostic instrument. Recent advancements in MRI analysis can address methodological challenges. Quantitative MRI and ultrasonographic techniques are employed to compare the material and structural qualities of adipose tissue in terms of durability, strength, and stability [6].

Accurate disease type detection need improved diagnostic methodologies, such as MRI. The diffusion process is a physical phenomenon resulting from the heat agitation of water molecules within the human body. The mobility of molecules is contingent upon the structure of the cellular tissue. The diffusion process can be delineated by MRI. This technique relies on the equipment design and the duration and amplitude of the applied magnetic field gradients associated with parameter [5].

3. RESEARCH METHODS

3.1. Connectivity Brain SEEG

The application of stereo electroencephalography with intracranial depth electrodes has facilitated the recording of brain activity throughout cortical, subcortical, and white matter regions. Surgeonally affixing SEEG electrodes in diverse orientations generates distinct stimulation dipoles in relation to the cortical axis. The presence of neurones at varying orientations yielded a range of response morphologies during SPES in SEEG, with orientations aligned to the cortical axis exhibiting more robust responses. The primary distinction between event-related responses (ERPs) to SPES captured using SEEG as pulse-evoked potentials (PEPs). The components of the SEEG PEP-like response exhibited increased variability, probably resulting from discrepancies in neuronal morphology and dipole orientation across the measured geographical locations. To recognise the fundamental distinctions between CCEP and SEEG PEPs, leveraging the relative temporal constraints associated with the detection of N1 and N2 to implement a uniform and automated detection methodology for identifying the initial two response components in SEEG SPES, designated as C1 and C2. Comparative analyses of SPES with alternative connection modalities have established a basis for correlating PEPs with recognised metrics of structural connectivity [2].

3.2. Method of SPES

SPES is employed on neural networks for functional brain mapping and seizure induction. This stimulation can elicit brain activity in areas associated with the stimulated site, thus facilitating the creation of connection atlases through large group analysis. Nonetheless, the precise delineation of such connection may be contingent upon the stimulation procedure [4].

Structural connectivity encompasses the physical connections between neurones, referred to as neuroanatomical connections, which pertain to white matter connectivity in the brain. Functional connectivity refers to the statistical interdependence of physiological time series obtained from several brain areas. Effective connection denotes the causal effect and direct influence of one brain part upon another. Functional and effective connection are ascertained through the sampling of signals documented throughout many temporal intervals that enhance comprehension of cerebral activity [3].

3.3. Data Electroencephalography Electrode

Invasive surgical insertion of 14 depth probes with a total of 152 electrode connections distributed across diverse anatomical sites in the right frontal and bilateral temporal regions. The

number of electrode contacts per probe varied from 8 – 16, with a median of 10 contacts. The SEEG probes possessed a diameter of 0.8 mm, with 8 – 16 electrode connections with a center-to-center distance of 3.5 mm, or a diameter of 1.28 mm with 9 recording contacts and a center-to-center distance of 5.0 mm between contacts [2].

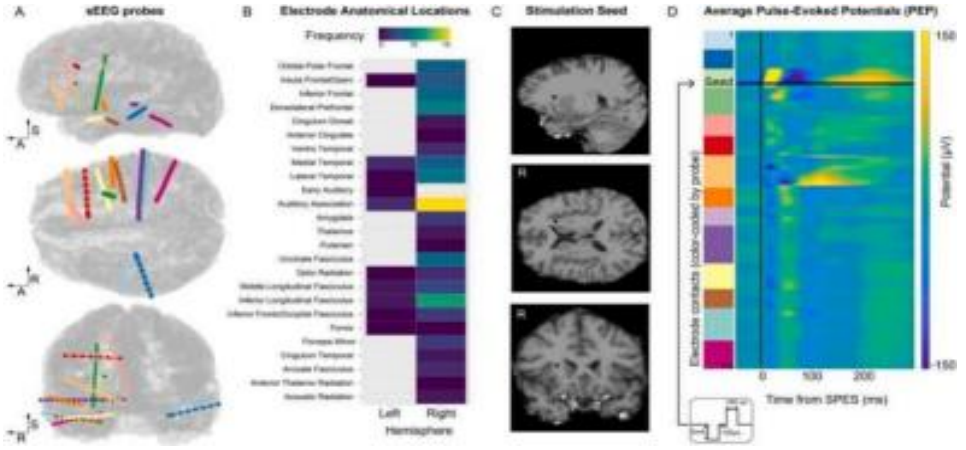

Figure 1. Summary of anatomical positioning and electrode stimulation. Illustrations: (A) quantity of electrode connections along the SEEG probe; (B) anatomical positioning of electrodes; (C) distinguished by the quantity of electrodes; and (D) comprehensive depiction of SEEG stimulation seed positions.

3.4. Anatomical Localisation of Electrode Placement in the Brain

The electrodes were identified using intracranial electrode visualisation software programs. Post-operative clinical CT images were acquired alongside pre-operative T1 anatomical MRI scans via a linear image registration method. The position of each electrode contact was manually determined on CT-MRI. The xyz coordinates for each electrode denote their spatial position (mm) in the R-A-convention. The coordinates of the S. electrode were obtained for anatomical labelling purposes. connections situated in cortical and subcortical regions were physically designated using a modified version of the volumetric HCPex atlas, while the HCP XTRACT probability was employed to name connections found in white matter. This stimulus localisation employed a monopolar cathode SPEC paradigm. A biphasic pulse with an amplitude of 5 mA and a width of 180 μs was administered to the designated electrode contact for stimulation using a Blackrock Cerestim R96 stimulator. The chosen electrode contact for stimulation acted as the stimulation seed. There were 315 single pulses with interstimulation durations that varied consistently between 400 ms and 1.2 d. The choice of stimulation seeds was driven by morphological and clinical factors. The SEEG probe was captured with a black Ceerebus 246 system at a sampling rate of 30 kHz with a high-pass filter applied. Signals were obtained from all electrode connections except the stimulated one. The recordings were correlated with electrode connections visibly seen in the white matter during the implantation operation. The quality of the SEEG signal was visually assessed for channel noise [2].

3.5. Magnetic Resonance Imaging

Diffusion-weighted imaging (DWI) data were obtained using a Siemens Prism system. The DWI data were analysed via the FSL diffusion toolbox. Fourteen volumes from the consolidated DWI data were utilised to estimate the field resulting from subject motion and distortions induced by eddy currents due to the application of rapid diffusion gradients, which were rectified using eddy software. Probability tractography reconstructs white matter pathways and elucidates structural connections non-invasively. Regions of interest (ROIs) were established for each electrode contact. A spherical mask with a radius of 2 mm is generated at the coordinates of the electrode. The spherical mask or stimulation seed is relocated from the initial pre-operative structural space to the original diffusion space using linear transformation. The resultant ROIs depict the stimulation field of the electrode contacts. Tractography is commenced and executed iteratively from each stimulation seed to all brain electrode sites [2].

4. RESULTS AND DISCUSSIONS

4.1. Model Conductance

Topology optimisation of electrically conductive material domains generates spatial conductivity maps that yield the ideal structural configuration for a system according to design objectives. Topology optimisation determines the optimal material distribution within a certain geometry. Topology optimisation utilised in electromagnetic metasurfaces represents an innovative application of topology optimisation in neuroscience, yielding straightforward physical models that facilitate the visualisation and comprehension of functional connectivity in the brain. Utilising specific coordinates of sEEG electrodes, a straightforward geometry is established comprising circular (2D) or spherical (3D) electrodes with a radius of 0.65 mm within a circular or spherical domain of 100 nm radius.

4.2. Correlation between PEP Physiology and Statistical Characteristics

Multiple PEP features were derived from the automated identification of C1 and C2 waveforms, as well as features from the averaged waveform captured at each site, utilising a high-pass filter to extract high-frequency waveforms. The time-dependent response components in the SPES SEEG exhibited inconsistency, necessitating the evaluation of various PEP features and their pairwise correlations. This analysis encompassed C1 and C2 peak amplitude, area, peak-to-peak distance, maximum amplitude, and RMS shape, resulting in a total of 21 pairs. The varied orientation of brain structures and the heterogeneous polarities produced at electrode contacts in SEEG identified the evoked components of C1 and C2 pulses based on latency rather than polarity. The polarities of C1 and C2 are antagonistic, whereas the components of N1 and N2 are present in CCEP. A robust association between the extracted matrices was established. Correlation coefficients varied from 0.96 to 0.67, with all p-values less than 0.0001. Variables exhibited a more consistent correlation with C1 peak amplitude and maximum amplitude. The RMS form exhibited diminished association with other factors. The consistency of correlation substantiates the choice of the C1 peak amplitude feature for modelling the correlation of PEP features. PEPs directed to distinct brain regions resulted in varying electrical potentials at the electrode contacts, exhibiting distinctive patterns for C1 values across electrode sites.

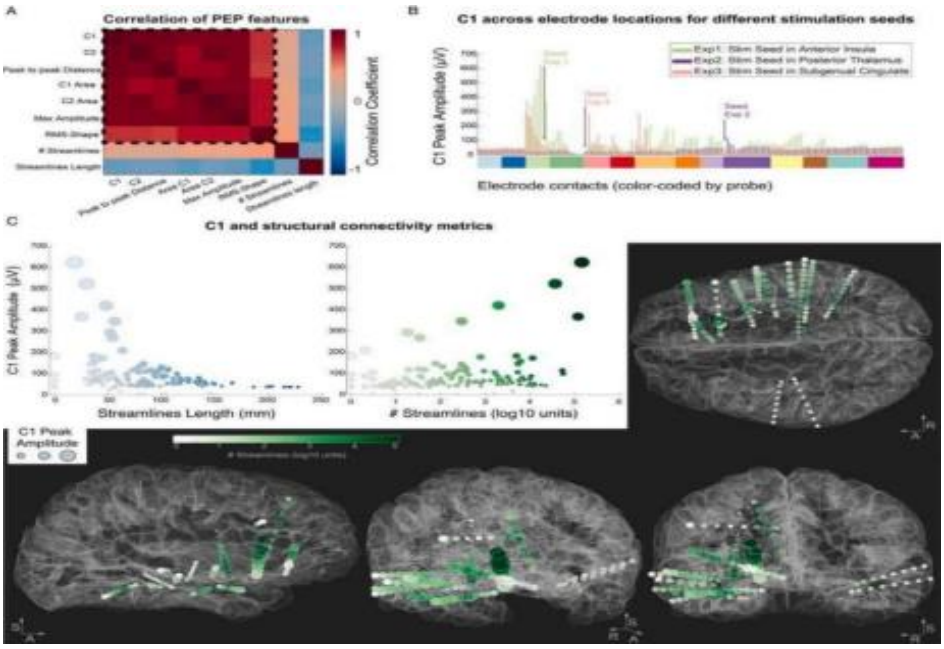

Figure 2. Correlations among PEP traits and their association with structural and anatomical data. Figures: (A) correlation matrix of all PEP feature pairs and structure matrix; (B) illustrates a comparison of C1 peak amplitude values at identical electrode sites; and (C) illustrates the correlation of C1 with the streamline matrix in tests demonstrating the exponential decay of C1.

4.3 Three-Dimensional Topological Model of Electrode Conductivity in Neural Structures

The design of the 3D domain network exhibits increased smoothness near the electrodes, resulting in high spatial resolution estimates of conductivity values at the proximal electrode sites. The limitation of the interpolated conductivity value is that the location is more distant from the cortical position of the sample. It subsequently presents a precise assessment of its structural data.

4.4 Error Location of Complex Anatomical Proximity Models

The evaluation of electrode positions exhibiting significant error was associated with anatomical organisation to assess and contrast diverse anatomical characteristics for each electrode site, encompassing proximity to the cortical surface, distance to the gray-white matter interface, and probability of close electrode contact with the sulcus as opposed to the gyrus. The correlation between anatomical characteristics and the 3D model was compromised by executing a median split of the dataset according to each anatomical feature. The distance from the cortical surface greatly influenced error, with electrodes nearer to the pial surface exhibiting greater model error. Electrodes positioned nearer to the sulcus exhibited a higher model error (17% compared to 10%, $z = 2.9$, $p = 0.004$).

The correlation between the level of structural connection and model error indicates that electrode contacts exhibit significant error when structural connectivity is weak or nonexistent. Outside the boundary of the sulcus, tractography inadequately identified grey matter regions owing to diminished diffusion anisotropy surrounding neuronal cell bodies and axon terminals. The ROI model for electrode contacts located in grey matter was reiterated for each stimulation seed, employing a 3 mm radius spherical mask to facilitate the tractography algorithm in recognising adjacent current lines, which exhibited significantly weaker directional consistency compared to white matter regions. The disparity in connectivity strength between the original and new ROI spherical mask sizes, along with model error, revealed that electrode contacts situated in grey matter regions with heightened connectivity likelihood ($n=29$) exhibited no statistically significant difference in model error compared to electrode contacts lacking an increased number of current lines ($n=40$; $z=0.6261$, $p=0.53$). These results indicate that this model may effectively assess connectivity to grey matter regions, in contrast to tractography, which exhibits reduced accuracy for pathways near the sulcus [2].

5. CONCLUSION

The findings indicate that SEEG is a technique that enables direct observation of cerebral activity via electrodes implanted into the brain. Although structural connectivity measurements can be accurately monitored using PEP characteristics, the amplitude of C1, indicative of effective connectivity, is not entirely represented by connectivity predicted using tractography or stimulation localisation with the monopolar cathode SPEC paradigm. Furthermore, the 3D domain network exhibits more uniform properties as it nears the electrode, resulting in enhanced conductivity values and superior resolution at the electrode's vicinity. These observations indicate a necessity for improved methodologies to augment the precision and resolution of brain connection assessments and stimulation procedures.

REFERENCES

[1] Nowinski, W. L. (2024). Storage estimation in morphology modeling of the human whole brain at the nanoscale. *Journal of Computational Science*, **81**, 102346.

[2] Schmid, W., Danstrom, I. A., Echevarria, M. C., Adkinson, J., Mattar, L., Banks, G. P., Sheth, S. A., Watrous, A. J., Heilbronner, S. R., Bijanki, K. R., Alabastri, A., & Bartoli, E. (2024). A biophysically constrained brain connectivity model based on stimulation-evoked potentials. *Journal of neuroscience methods*, **405**, 110106.

[3] Jedynak, M., Boyer, A., Mercier, M., Chanteloup-Forêt, B., Bhattacharjee, M., Kahane, P., David, O., & F-TRACT Consortium. (2024). SEEG electrode shaft affects amplitude and latency of potentials evoked with single pulse electrical stimulation. *Journal of Neuroscience Methods*, **403**, 110035.

[4] Ismail, L. E. & Karwowski, W. (2020). A graph theory-based modeling of functional brain connectivity based on EEG: a systematic review in the context of neuroergonomics. *IEEE Access*, **8**, 155103–155135.

[5] Ortiz-Abellán, C., Aguado-Sarrió, E., Prats-Montalbán, J. M., Camps-Herrero, J., & Ferrer, A. (2024). New breast cancer biomarkers from diffusion magnetic resonance imaging based on the Diffusion Tensor using multivariate curve resolution (MCR) models. *Chemometrics and Intelligent Laboratory Systems*, **251**, 105171.

[6] Monte, A., Skypala, J., Vilimek, D., Juras, V., & Jandacka, D. (2023). Correlations between Achilles tendon material and structural properties and quantitative magnetic resonance imagining in different athletic populations. *Journal of biomechanics*, **159**, 111796.